COMMUNICATION

Reusable polymer brush-based photocatalysts for PET-RAFT polymerization

Received 00th January 20xx,
Accepted 00th January 20xx

DOI: 10.1039/x0xx00000x

Kirsten Bell[a], Sarah Freeburne[a], Adam Wolford[a], Christian W. Pester[*a,b]

This contribution discusses the control over polymerization using a heterogeneous photocatalyst based on fluorescein polymer brushes tethered to micron-scale glass supports (FPB@SiO_2). FPB@SiO_2-catalyzed photoinduced electron/energy transfer-reversible addition-fragmentation chain transfer (PET-RAFT) polymerization is shown to provide high conversions, controlled molecular weights and narrow molecular weight distributions for a variety of monomers. Moreover, the beads can catalyze PET-RAFT on gram scales, in the presence of oxygen, while allowing full catalyst recovery through simple filtration. Finally, their high shelf-life allows for multiple polymerizations and user-friendly access to precision macromolecules under mild reaction conditions even after prolonged (months) storage time.

Introduction

By enabling chemical transformations under ambient conditions and visible light irradiation, photoredox catalysis has significantly impacted polymer chemistry.[1–11] Reversible deactivation radical polymerizations (RDRPs) of a wide range of monomers can now be performed at room temperature and in the presence of ambient oxygen via visible light-mediated atom transfer radical polymerization (ATRP),[12–15] photoinduced electron/energy transfer reversible addition-fragmentation chain transfer (PET-RAFT),[16–26] or photoiniferter-mediated polymerization.[27,28] Many reported light-mediated RDRPs use homogeneous catalysis approaches,[1,4,5,7,12,29,30] which invariably entails a potential for catalyst contamination. This can lead to discoloration or degradation of the synthetic products.[12,29,31–33]

Heterogeneous photocatalysis is a viable alternative:[34–41] the ability to reuse catalysts for multiple reactions mitigates catalyst impurities, and improves both sustainability and cost effectiveness considering the often prohibitively expensive nature of some (e.g., $Ir(ppy)_3$).[12,18] Recent heterogeneous photocatalytic systems have been based on nanoparticles,[42–51] polymer networks,[52–67] metal oxides,[68–72] or catalytic (single chain nanoparticle) polymers.[73,74] However, nanoparticles themselves strongly absorb visible light and reduce light penetration into the reaction mixture. Further, centrifugation is required for product purification, inherently limiting scalability.[75] For photocatalytic networks (polymeric or metal organic), infiltration of the network with reactants and products can limit reusability. Finally, polymeric catalysts are inherently difficult to separate from polymeric products. Such challenges create a necessity for new and user-friendly approaches to leverage the full potential of heterogeneous photocatalysis on larger scales.

Here, we attempt to address these limitations by introducing photocatalyst polymer brush-functionalized glass beads as heterogeneous photopolymerization catalysts (PC@SiO_2). The micron-size transparent SiO_2 supports assure improved light penetration throughout the reaction mixture and afford facile recovery through filtration and reuse for multiple consecutive reactions. PC@SiO_2-catalyzed PET-RAFT polymerization is shown to be oxygen tolerant, provides temporal control (on/off), and synergistic with various monomer families to produce well-defined polymers with low dispersity. Finally, a long shelf-life of the catalysts (over months) indicates long-term stability. While fluorescein-functionalized polymer brushes are used as a model photocatalyst herein, this platform can readily be extended towards other tethered photocatalysts and other photocatalytic conversions.

Results and Discussion

Fluorescein polymer brush glass beads (FPB@SiO_2, **Figure 1a**) were synthesized following our previously published procedure.[76] Successful surface functionalization was verified via X-ray photoelectron spectroscopy (XPS) and thermal gravimetric analysis (TGA, see supporting information **Figure S4**). As shown

[a] *Department of Chemical Engineering, The Pennsylvania State University, University Park, PA 16802, USA.*
[b] *Department of Chemistry, Department of Materials Science and Engineering, The Pennsylvania State University, University Park, PA 16802, USA.*

Electronic Supplementary Information (ESI) available. See DOI: 10.1039/x0xx00000x

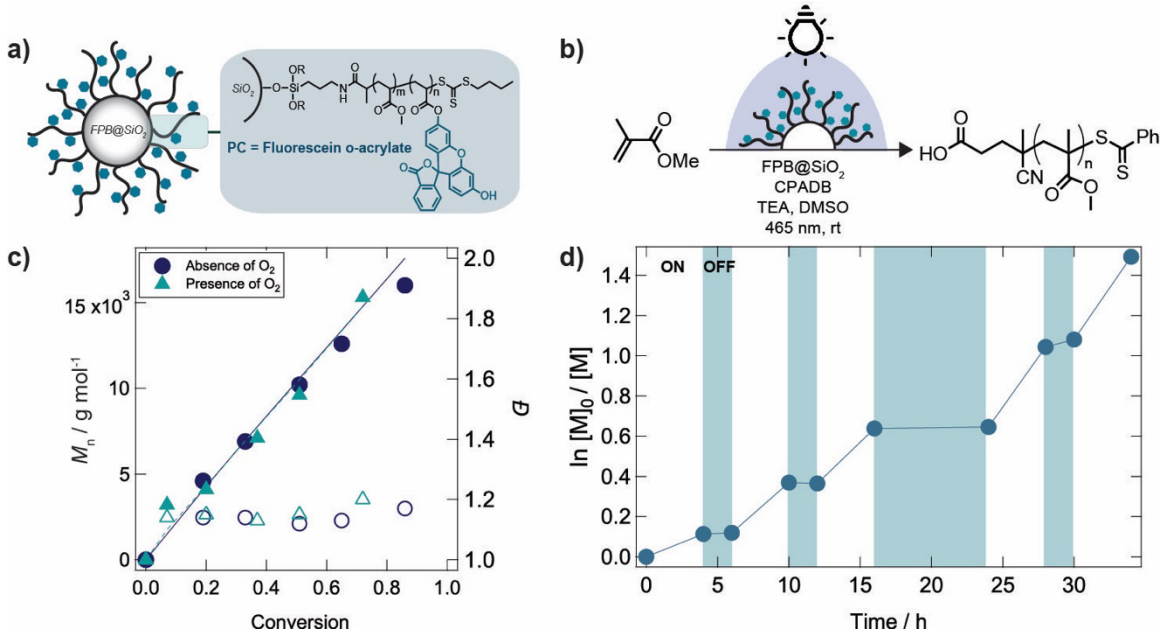

Figure 1. (a) Illustration of poly(fluorescein *o*-acrylate-*co*-methyl acrylate) polymer brush beads (FPB@SiO_2) and (b) light-mediated reversible addition-fragmentation chain transfer (RAFT) of methyl methacrylate (MMA). (c) Kinetic analysis of PET-RAFT polymerization of MMA using 20% FPB@SiO_2 shows a linear increase in molecular weight (M_n) with conversion both in the absence and presence of oxygen. (d) Monomer conversion, $\ln[M]_0/[M]$ with time while toggling the light source on/off indicates temporal control.

in **Figure 1**, FPB@SiO_2 catalysts provide excellent control over PET-RAFT of methyl methacrylate (MMA) under blue light irradiation (λ_{max} = 465 nm) using 4-cyano-4-(phenylcarbonothioylthio)pentanoic acid (CPADB) as the chain transfer agent (CTA) in dimethyl sulfoxide (DMSO), and with triethyl amine (TEA, sacrificial electron donor) at a ratio of [MMA]:[CPADB]:[PC]:[TEA] = 200:1:0.021:1. Theoretical and experimental molecular weights as determined by gel permeation chromatography (GPC) were in good agreement. Conversion increased linearly with exposure time and confirmed the controlled characteristics of PET-RAFT. Monomer conversions reached >90% and PMMA of M_n = 20,400 g mol^{-1} was obtained while maintaining low dispersities throughout ($Đ$ < 1.3). Higher PMMA molecular weights (M_n = 66,700 g mol^{-1}) were possible by increasing the monomer to CTA ratio, despite MMA's low propagation rate constant (k_p), and increasing viscosity with the PC@SiO_2 beads in the polymerization solution.[77,78] Mass transport limitations can increase termination events and lead to challenges in achieving ultra-high molecular weights (10^6 g mol^{-1}). For the present system, addition of solvent failed to achieve higher degrees of polymerizations (see **Table S1**). It is noteworthy that optimization of catalyst grafting densities, FPB polymer brush thickness, as well as particle diameters are few of many experimental factors that we anticipate could increase the maximum attainable molecular weight. Current efforts in our group are working towards systematically interrogating these catalyst-system parameters and overcoming mass transport limitations. Nonetheless, molecular weights with the present approach are well-controlled and successful scale-up was possible to produce PMMA on the gram-scale (84% conversion after 24 hours, $M_{n,PMMA}$ = 15,700 g mol^{-1}, $Đ$ = 1.24).

Polymerization inherently was successful both in closed vials without prior deoxygenation as well as in vessels fully open to air (see **Figure 1c and Figure S8**). However, a low molecular weight tail in the ultraviolet (UV) GPC elution traces was present when PMMA was polymerized in the presence of oxygen (**Figure S10**). While control experiments in ambient atmospheres showed improved dispersities for PMMA (**Table S2**), chain end fidelity and control over polymerization are reduced. Due to superior control and kinetics in inert conditions, experiments described throughout the remainder of this contribution were conducted under N_2. **Table S1** provides additional details the role of various experimental parameters to improve mass transport and enable higher monomer conversions.

Figure 1d indicates successful temporal control over FPB@SiO_2-catalyzed PET-RAFT by toggling the light source "ON" and "OFF" with no minimal conversion in the dark.[79]

The FPB@SiO_2 heterogeneous catalysts were determined to be shelf-stable for over 60 days when stored in the dark and in the presence of oxygen. After 63 days, monomer conversion reached 85% (24 h reaction time) to yield PMMA with M_n = 16,100 g mol^{-1} and narrow $Đ$ = 1.15. No change in catalytic activity was observed compared to freshly prepared FPB@SiO_2 (83% MMA conversion after 24h, M_n = 16,900 g mol^{-1}, $Đ$ = 1.16).

Table 1 outlines control experiments that indicated minimal polymerization in the absence of photocatalyst (entry 1) or when using plain, unfunctionalized SiO_2 beads (entry 2). Low monomer conversions (11% and 6%, respectively) are in agreement with the CPADB CTA's ability to act as a photoiniferter.[27,28,80] Without the CPADB, free radical polymerization occurred to give PMMA with broad molecular weight distribution ($Đ$ = 3.56, entry 3). In the absence of TEA (entry 4), polymerization was found to be significantly slower, confirming TEA's reported supportive role as a sacrificial electron donor.[22] Finally, no polymerization occurred in the absence of irradiation (entry 5).

Table 1. Control experiments for the PET-RAFT polymerization of MMA

Entry	Experimental Conditions[a]	Conv.[b]	$M_{n,\,Theo}$ (g mol^{-1})	$M_{n,\,GPC}$[c] (g mol^{-1})	$Đ$[c]
1[d]	200:1:0:1	11%	3,900	2,500	1.2
2[e]	200:1:0:1	6%	2,500	1,500	1.27
3[f]	200:0:0.015:1	13%	3,000	9,500	3.56
4[f]	200:1:0.015:0	9%	2,000	2,100	1.29
5[g]	200:1:0.015:1	0%	-	-	-

All polymerizations were performed in the absence of O_2 in DMSO at RT under (λ_{max} = 465 nm LED irradiation for 16 h. [a]Experiments were performed at a ratio of [MMA]:[CPADB]:[PC]:[TEA]. [b]Monomer conversion determined by ^{1}H NMR. [c]M_n and $Đ$ determined via GPC in THF using universal calibrations. [d]No photocatalyst was added to reaction. [e]~1,500 mg plain, unfunctionalized beads used in polymerization. [f]~1,500 mg FPB@SiO_2 beads used. [g]Reaction performed in the dark with ~1,500 mg FPB@SiO_2 beads.

Because the photocatalyst is covalently tethered to the SiO_2 support, catalyst impurities in the final products are reduced and purification is facilitated. Neither ultraviolet-visible (UV-vis) spectroscopy nor Fourier-transform infrared spectroscopy (FT-IR) indicated any leaching of fluorescein into the reaction solution (**Figure S6a and S6b**). Fluorescein's distinct absorption λ_{max} = 279 nm (in DMSO) was absent and FT-IR spectra showed no noticeable aromatic C=C stretch (1590 cm^{-1}) for representative PMMA samples. FPB@SiO_2 beads were also stirred in various solvents to determine if e.g., hydrolysis[81–83] of the surface-tethered polymer brushes can occur to contaminate the reaction mixture. After stirring FPB@SiO_2 in DMSO for an extended time of 7 days, ^{1}H nuclear magnetic resonance (NMR) spectra indicated only trace amounts of aromatic peaks from fluorescein and minimal leaching of photocatalytic polymer brushes into the solution (**Figure S17a**). In contrast, stirring FPB@SiO_2 in water indeed shows significant hydrolysis and contamination (**Figure S17b**). As such, the choice of solvents that cannot hydrolyse the R_3-Si-O tether is important to obtain pure products.

Simple filtration allows for removal of the micron-size FPB@SiO_2 catalysts from the reaction solution and reuse for up to seven subsequent PET-RAFT polymerizations (see **Figure 2**).

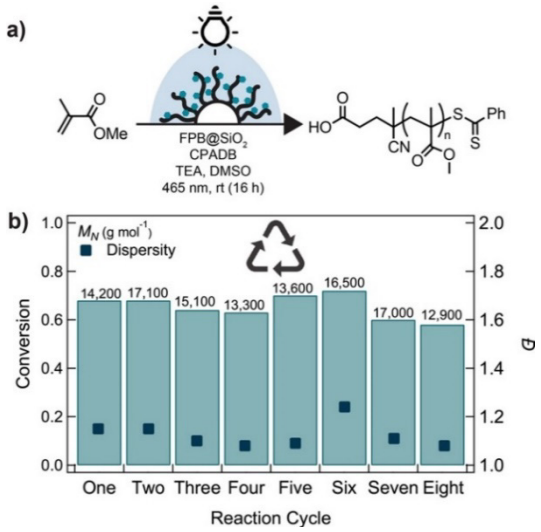

Figure 2. (a) PET-RAFT of methyl methacrylate (MMA) using FPB@SiO_2. (b) FPB@SiO_2 catalysts were recycled while providing reproducible molecular weights, monomer conversions, and dispersities.

After 16 h, all polymerization reached similar conversions (65.4 ± 4.9%) and PMMA molecular weights (15,000 ± 1700 g mol^{-1}) and dispersities (1.13 ± 0.05) indicated good retention of FPB@SiO_2 photocatalytic activity throughout multiple uses and cleaning steps.

Mechanistically, polymerization is anticipated to follow the established PET-RAFT process.[16,18,22] The fluorescein photocatalyst (PC) within the polymer brush is excited by light and undergoes an electron transfer with the CTA to initiate polymerization (**Figure 3**). In the presence of an electron donor (ED, Et_3N), a reductive quenching pathway is favored, producing a radical anion (PC$^{\bullet}$) that enables photoelectron transfer with the CTA.[16,46] Recombination to recover the dormant RAFT polymer chain occurs through interaction of a radical chain end with a PC at the same or a different PC@SiO_2 particle. Additional experiments to unravel the precise nature of this heterogeneous process are subject to further work in our group.

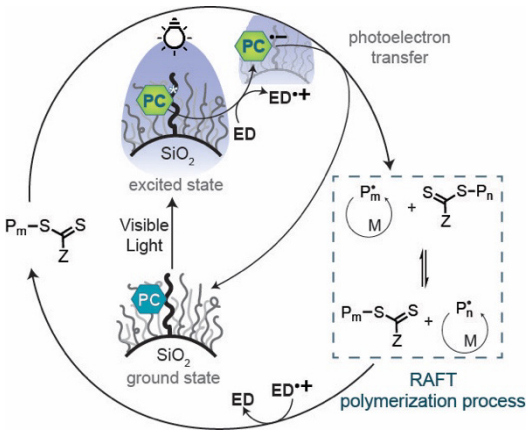

Figure 3. Proposed mechanism for PET-RAFT (reductive quenching cycle) catalyzed by FPB@SiO_2 photocatalysts in the presence of a sacrificial electron donor (ED).

It is worth commenting on the choice of fluorescein as the photocatalyst as other organic photocatalysts (e.g., Eosin Y) have shown better PET-RAFT performance in studies by other groups.[22] Following a literature procedure,[84] we synthesized EY monomers and EY@SiO_2 catalysts (see SI). PET-RAFT of MMA with EY@SiO_2 indeed achieved higher monomer conversion than FPB@SiO_2: 75% after 16 h to give PMMA with $M_{n,GPC}$ = 22,000 g mol^{-1} and $Đ$ = 1.15. However, when recycled just once, conversion for the second polymerization decreased to 47% ($M_{n,GPC}$ = 7,800 g mol^{-1} , $Đ$ = 1.1). We hypothesize that this lower conversion results from photobleaching and degradation of EY@SiO_2 (see **Figure S18**).[85] Indeed, studies have shown that Eosin-Y is prone to photobleach more readily.[86–88] This is also clearly visible to the naked eye when comparing the colours of the EY@SiO_2 beads before and after the first polymerization (see **Figure S18**)

We further studied whether the SiO_2-tethered CTA chain end can detach and incorporate monomer into the backbone of the fluorescein polymer brush during the PET-RAFT process. To interrogate this, XPS was performed on the FPB@SiO_2 catalysts after the polymerization of 2,2,2-trifluoroethyl methacrylate (TFEMA, **Figure S22c**). Appearance of fluorine F1s peak at BE_{F1s} = 689 eV indicated that the surface-anchored BTPA chain ends

indeed add monomer into the polymer brush structure during bulk polymerization. Even following CTA chain end removal attempts, fluorine was still present (albeit at lower quantities: 3% vs. 5%), indicating chain end removal may not occur to full conversion or physisorption of solution polymer onto the beads is occurring. Nevertheless, it is important to note that there was no negative effect of this on PET-RAFT polymerization kinetics when comparing chain end-removed vs. native FPB@SiO_2 catalysts (**Figure S22a** and **b**).

The described FPB@SiO_2 approach requires lower catalyst loadings and achieved higher conversions when compared to published work on fluorescein as a homogeneous PET-RAFT catalyst.[37,22,23] Furthermore, the described approach is easy to use and does not require great precision with respect to weighing out the exact amount of required catalyst. Different concentrations of FPB@SiO_2 were investigated, ranging from 5 ppm to 500 ppm (**Figure S19a**) to identify the required catalyst loading, i.e., bead amount, to achieve controlled polymerization of MMA. Notably, similar polymerization results were obtained irrespective of PC@SiO_2 catalyst amount added to the reaction mixture. Previous photopolymerization studies have indicated that an exceedingly high catalyst concentration can be detrimental to reaction control.[89] To investigate this, an equivalent fluorescein molar amount per milligram bead was determined through TGA (~4.46 x 10^{-7} mmol fluorescein per mg glass bead, **Figure S4b**). Indeed, for a 500 ppm FPB@SiO_2 loading, polymerizations were well-defined initially, but an increasing dispersities and discrepancy between theoretical and experimental molecular weight at later stages indicates loss of control (**Figure S19b**). Decreasing the FPB@SiO_2 loading to 140 ppm significantly improved both dispersity and consistency between experimental and theoretical molecular weights (**Figure S19b**). However, further decreasing the fluorescein loading decreased the polymerization rate (**Figure S19a** and **Figure S20**).

Table 2. FPB@SiO2-catalyzed PET-RAFT polymerization results for different monomers.

	Monomer	Time (hr)	Conv.[a]	$M_{n,\,theo}$ (g mol^{-1})	$M_{n,\,GPC}$[b] (g mol^{-1})	$Đ$[b]
1	BnMA[e]	12	81%	28,900	27,200	1.29
2	TFEMA[e]	16	77%	26,000	27,300	1.25
3	PEGMEMA[e]	16	62%	37,700	26,200	1.27
4	MA[f]	16	80%	14,100	12,900	1.16
5	BA[f]	16	67%	17,200	16,500	1.12
6	DMA[f]	16	75%	15,100	11,300[c]	1.08[d]
7	DEA[f]	16	97%	24,600	10,200	1.2

Reactions were performed in the absence of O_2 in DMSO at RT under λ_{max} = 465 nm LED light with ~1,150 mg FPB@SiO_2 with a 200:1 [M]:[CTA] ratio. [a]Monomer conversion determined by ^{1}H NMR. [b]M_n and $Đ$ determined through GPC in THF using universal calibrations. [c]M_n determined through chain-end analysis using ^{1}H-NMR and [d]dispersity ($Đ$) determined through SEC in DMF. [e]CPADB, [f]DDMAT.

FPB@SiO_2 can catalyze PET-RAFT of other methacrylates, acrylates, and acrylamides. **Table 2** highlights good agreement between targeted and experimental molecular weights while maintaining low dipersities for: benzyl methacrylate (BnMA), poly(ethylene glycol)methyl ether methacrylate (PEGMEMA), methyl acrylate (MA), butyl acrylate (BA), *N*,*N*-dimethylacrylamide (DMA), and *N*,*N*-diethylacrylamide (DEA). RAFT CTAs were chosen based on their reported monomer compatibility:[25] CPADB for methacrylates and 2-(dodecylthiocarbonothioylthio)-2-methylpropionic acid (DDMAT) for acrylates and acrylamides.

Finally, chain extensions using PMA (M_n = 11,100 g mol^{-1} and $Đ$ = 1.16) and PMMA (M_n = 16,00 g mol^{-1} and $Đ$ = 1.09, see **Figure S24)** as macroinitiators were performed to confirm the presence of the CTA end group. **Figure 4** and **Figure S24** show successful polymer chain extension through PET-RAFT polymerization of butyl acrylate and benzyl methacrylate respectively. While low molecular weight tailing in GPC suggests loss of some macroinitiator chain ends, mass spectroscopy via MALDI-TOF suggests the PMA macroinitiator does not suffer from any significant loss of the DDMAT chain ends (**Figure S29**). Furthermore, the resulting poly(MA-*b*-BA) diblock copolymer clearly showed increased molecular weight (M_n = 29,600 g mol^{-1}, $Đ$ = 1.21). Similarly, poly(MMA-*b*-BnMA) also indicated an increase of molecular weight (M_n = 36,500 g mol^{-1} and $Đ$ = 1.27). The characteristic peaks of the respective block copolymers of BA and BnMA were confirmed through ^{1}H NMR (**Figure S31** and **S38**).

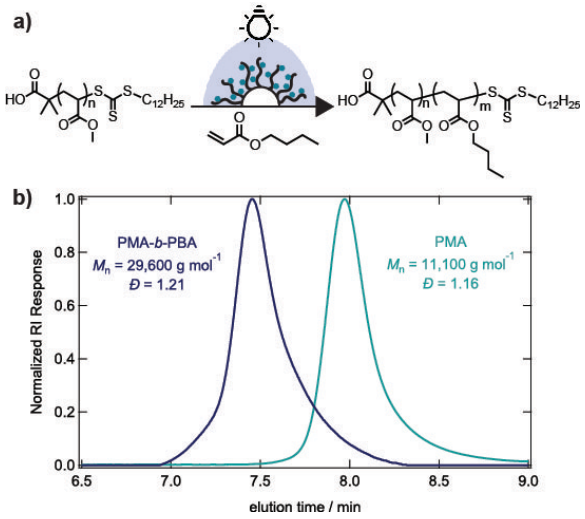

Figure 4. Chain extension of (a) poly(methyl acrylate) (PMA) macro-chain transfer agents with butyl acrylate (BA). (b) The normalized GPC trace indicating the growth of PMA-*block*-PBA diblock copolymers.

Conclusions

This work introduced a robust heterogeneous photoredox polymerization catalyst system based on fluorescein functionalized polymer brush glass beads (FPB@SiO_2). FPB@SiO_2-catalyzed PET-RAFT polymerization of a variety of monomers in the presence of oxygen was shown to provide well-controlled molecular weights and dispersities. The FPB@SiO_2 approach enabled low catalyst loadings and showed the potential to be recycled for multiple consecutive polymerizations after simple filtration. After filtration, the catalysts remain stable and showed good shelf-life and control over polymerization even after extended storage over months. Due to the covalent tether of the photocatalyst to the SiO_2 support, catalyst contamination in the

final polymer product could minimized. Finally, block copolymerization studies indicated appropriate chain end fidelity despite some low molecular weight tailing. Future studies in our laboratory are aimed at enhancing this heterogeneous photocatalysis platform towards other catalysts and chemical reactions.

Author Contributions

All authors approved the final version of the manuscript.

Corresponding Author

*pester@psu.edu

Acknowledgements

C.W.P. acknowledges the NSF for financial support. The authors would like to thank T. J. Zimudzi (PSU Materials Characterization Lab) for assistance with UV-vis and FT-IR and both E. Llyod and Prof. R. Hickey from for assistance with obtaining SEC data. The authors thank Dr. Tatiana Laremore and Dr. Sergei Koshkin for performing mass spectrometric analysis on polymer samples.

Funding sources

National Science Foundation (NSF CBET Award # 2143628).

Notes and references

1 M. Chen, M. Zhong and J. A. Johnson, *Chem Rev*, 2016, **116**, 10167–10211.

2 S. Chatani, C. J. Kloxin and C. N. Bowman, *Polym Chem*, 2014, **5**, 2187–2201.

3 X. Pan, M. A. Tasdelen, J. Laun, T. Junkers, Y. Yagci and K. Matyjaszewski, *Prog Polym Sci*, 2016, **62**, 73–125.

4 S. Shanmugam and C. Boyer, *Science*, 2016, **352**, 1053–1054.

5 N. Corrigan, J. Yeow, P. Judzewitsch, J. Xu and C. Boyer, *Angew Chem Int Ed* `, 2019, **58**, 5170–5189.

6 N. Corrigan, S. Shanmugam, J. Xu and C. Boyer, *Chem Soc Rev*, 2016, **45**, 6165–6212.

7 J. T. Trotta and B. P. Fors, *Synlett*, 2016, **27**, 702–713.

8 L. M. M. Pascual, A. E. Goetz, A. M. Roehrich and A. J. Boydston, *Macromol Rapid Commun*, 2017, **38**, 1–6.

9 V. Kottisch, Q. Michaudel and B. P. Fors, *J Am Chem Soc*, 2016, **138**, 15535–15538.

10 Y. Yagci, S. Jockusch and N. J. Turro, *Macromolecules*, 2010, **43**, 6245–6260.

11 S. Shanmugam, J. Xu and C. Boyer, *Macromol Rapid Commun*, 2017, **38**, 1–40.

12 N. J. Treat, H. Sprafke, J. W. Kramer, P. G. Clark, B. E. Barton, J. Read De Alaniz, B. P. Fors and C. J. Hawker, *J Am Chem Soc*, 2014, **136**, 16096–16101.

13 B. P. Fors and C. J. Hawker, *Angew. Chem Int Ed*, 2012, **51**, 8850–8853.

14 R. M. Pearson, C. H. Lim, B. G. McCarthy, C. B. Musgrave and G. M. Miyake, *J Am Chem Soc*, 2016, **138**, 11399–11407.

15 J. C. Theriot, B. G. McCarthy, C. H. Lim and G. M. Miyake, *Macromol Rapid Commun*, 2017, **38**, 1–12.

16 M. L. Allegrezza and D. Konkolewicz, *ACS Macro Lett*, 2021, **10**, 433–446.

17 S. Li, G. Han and W. Zhang, *Polym Chem*, 2020, **11**, 1830–1844.

18 J. Phommalysack-Lovan, Y. Chu, C. Boyer and J. Xu, *Chem Comm*, 2018, **54**, 6591–6606.

19 N. Corrigan, D. Rosli, J. Warren Jeffrey Jones, J. Xu and C. Boyer, *Macromolecules*, 2016, **49**, 6779.

20 C. A. Figg, J. D. Hickman, G. M. Scheutz, S. Shanmugam, R. N. Carmean, B. S. Tucker, C. Boyer and B. S. Sumerlin, *Macromolecules*, 2018, **51**, 1370–1376.

21 C. Wu, N. Corrigan, C. H. Lim, K. Jung, J. Zhu, G. Miyake, J. Xu and C. Boyer, *Macromolecules*, 2019, **52**, 236–248.

22 J. Xu, S. Shanmugam, H. T. Duong and C. Boyer, *Polym Chem*, 2015, **6**, 5615–5624.

23 Y. Song, Y. Kim, Y. Noh, V. K. Singh, S. K. Behera, A. Abudulimu, K. Chung, R. Wannemacher, J. Gierschner, L. Lüer and M. S. Kwon, *Macromolecules*, 2019, **52**, 5538–5545.

24 B. Nomeir, O. Fabre and K. Ferji, *Macromolecules*, 2019, **52**, 6898–6903.

25 G. Ng, K. Jung, J. Li, C. Wu, L. Zhang and C. Boyer, *Polym Chem*, 2021, **12**, 6548–6560.

26 V. Bellotti and R. Simonutti, *Polymers*, 2021, **13**, 7, 1119.

27 T. G. McKenzie, Q. Fu, E. H. H. Wong, D. E. Dunstan and G. G. Qiao, *Macromolecules*, 2015, **48**, 3864–3872.

28 J. Xu, S. Shanmugam, N. A. Corrigan and C. Boyer, *Controlled Radical Polymerization: Mechanisms*, 2015, **Ch. 13**, 247–267.

29 K. Schröder, K. Matyjaszewski, K. J. T. Noonan and R. T. Mathers, *Green Chem*, 2014, **16**, 1673–1686.

30 J. C. Theriot, B. G. McCarthy, C. H. Lim and G. M. Miyake, *Macromol Rapid Commun*, 2017, **38**, 1–12.

31 N. V. Tsarevsky and K. Matyjaszewski, *Chem Rev*, 2007, **107**, 2270–2299.

32 C. Wu, S. Shanmugam, J. Xu, J. Zhu and C. Boyer, *Chem Comm*, 2017, **53**, 12560–12563.

33 G. A. Epling and C. Lin, *Chemosphere*, 2002, **46**, 561–570.

34 T. Fulgheri, F. Della Penna, A. Baschieri and A. Carlone, *Curr Opin Green Sustain Chem*, 2020, **25**, 100387.

35 J. Qiu, B. Charleux and K. Matyjaszewski, *Prog Polym Sci*, 2001, **26**, 2083–2134.

36 Y. Chu, Z. Huang, K. Liang, J. Guo, C. Boyer and J. Xu, *Polym Chem*, 2018, **9**, 1666–1673.

37 A. Savateev and M. Antonietti, *ACS Catal*, 2018, **8**, 9790–9808.

38 J. Z. Bloh and R. Marschall, *Eur J Org Chem*, 2017, **2017**, 2085–2094.

39 Z. An, S. Zhu and Z. An, *Polym Chem*, 2021, **12**, 2357–2373.

40 D. M. Haddleton, D. J. Duncalf, D. Kukulj and A. P. Radigue, *Macromolecules*, 1999, **32**, 4769–4775.

41 Q. Fu, T. G. McKenzie, J. M. Ren, S. Tan, E. Nam and G. G. Qiao, *Sci Rep*, 2016, **6**, 1–12.

42 R. Chen, Z. Jalili and R. Tayebee, *RSC Adv*, 2021, **11**, 16359–16375.

43 M. M. Khani, Z. M. Abbas and B. C. Benicewicz, *J Polym Sci A Polym Chem*, 2017, **55**, 1493–1501.

44 B. Martins Estevão, F. Cucinotta, N. Hioka, M. Cossi, M. Argeri, G. Paul, L. Marchese and E. Gianotti, *Phys Chem Chem Phys*, 2015, **17**, 26804–26812.

45 G. M. Scheutz, J. Elgoyhen, K. C. Bentz, Y. Xia, H. Sun, J. Zhao, D. A. Savin and B. S. Sumerlin, *Polym Chem*, 2021, **12**, 4462–4466.

46 S. Shanmugam, S. Xu, N. N. M. Adnan and C. Boyer, *Macromolecules*, 2018, **51**, 779–790.

47 J. Wang, M. Rivero, A. Muñoz Bonilla, J. Sanchez-Marcos, W. Xue, G. Chen, W. Zhang and X. Zhu, *ACS Macro Lett*, 2016, **5**, 1278–1282.

48 J. Woo, H. Park, Y. Na, S. Kim, W. Il Choi, J. H. Lee, H. Seo and D. Sung, *RSC Adv*, 2020, **10**, 2998–3004.

49 K. P. McClelland, T. D. Clemons, S. I. Stupp and E. A. Weiss, *ACS Macro Lett*, 2020, **9**, 7–13.

50 Y. Huang, X. Li, J. Le Li, B. Zhang and T. Cai, *Macromolecules*, 2018, **51**, 7974–7982.

51 J. Jiang, G. Ye, Z. Wang, Y. Lu, J. Chen and K. Matyjaszewski, *Angew Chem*, 2018, **130**, 12213–12218.

52 M. Chen, S. Deng, Y. Gu, J. Lin, M. J. MacLeod and J. A. Johnson, *J Am Chem Soc*, 2017, **139**, 2257–2266.

53 J. X. Jiang, Y. Li, X. Wu, J. Xiao, D. J. Adams and A. I. Cooper, *Macromolecules*, 2013, **46**, 8779–8783.

54 W. L. Guo, Y. Zhou, B. Duan, W. F. Wei, C. Chen, X. Li and T. Cai, *Chem Eng J*, 2022, **429**, 132120.

55 X. Li, Y. C. Zhang, S. Ye, X. R. Zhang and T. Cai, *J Mater Chem A Mater*, 2020, **8**, 25363–25370.

56 X. Li, Y. C. Zhang, Y. Zhao, H. P. Zhao, B. Zhang and T. Cai, *Macromolecules*, 2020, **53**, 1550–1556.

57 Y. Liang and D. E. Bergbreiter, *Polym Chem*, 2016, **7**, 2161–2165.

58 Z. Lu, H. Yang, X. Fu, Y. Zhao, L. Xiao, Z. Zhang and L. Hou, *Macromol Rapid Commun*, 2021, **42**, 1–8.

59 S. M. Soria-Castro, B. Lebeau, M. Cormier, S. Neunlist, T. J. Daou and J. P. Goddard, *Eur J Org Chem*, 2020, **2020**, 1572–1578.

60 A. Sridhar, R. Rangasamy and M. Selvaraj, *New J Chem*, 2019, **43**, 17974–17979.

61 Z. J. Wang, K. Landfester and K. A. I. Zhang, *Polym Chem*, 2014, **5**, 3559–3562.

62 Z. Y. Xu, Y. Luo, D. W. Zhang, H. Wang, X. W. Sun and Z. T. Li, *Green Chemistry*, 2020, **22**, 136–143.

63 K. Zhang, Z. Vobecka, K. Tauer, M. Antonietti and F. Vilela, *Cheml Comm*, 2013, **49**, 11158–11160.

64 Y. Zhu, D. Zhu, Y. Chen, Q. Yan, C. Y. Liu, K. Ling, Y. Liu, D. Lee, X. Wu, T. P. Senftle and R. Verduzco, *Chem Sci*, 2021, **12**, 16092–16099.

65 C. A. Wang, Y. W. Li, X. L. Cheng, J. P. Zhang and Y. F. Han, *RSC Adv*, 2017, **7**, 408–414.

66 S. Dadashi-Silab, F. Lorandi, M. J. DiTucci, M. Sun, G. Szczepaniak, T. Liu and K. Matyjaszewski, *J Am Chem Soc*, 2021, **143**, 25, 9630-9638.

67 C. G. Wang, J. J. Chang, E. Y. J. Foo, H. Niino, S. Chatani, S. Y. Hsu and A. Goto, *Macromolecules*, 2020, **53**, 51–58.

68 Y. Huang, X. R. Zhang, S. Ye, J. Le Li, X. Li and T. Cai, *Nanoscale*, 2019, **11**, 13502–13510.

69 X. Li, S. Ye, Y. C. Zhang, H. P. Zhao, Y. Huang, B. Zhang and T. Cai, *Nanoscale*, 2020, **12**, 7595–7603.

70 Y. Liu, B. Li, H. S. Li, P. Wu and J. Wang, *Dalton Trans*, 2020, **49**, 17520–17526.

71 L. Zhang, X. Shi, Z. Zhang, R. P. Kuchel, R. Namivandi-Zangeneh, N. Corrigan, K. Jung, K. Liang and C. Boyer, *Angew Chem Int Ed*, 2021, **60**, 5489–5496.

72 K. Hakobyan, T. Gegenhuber, C. S. P. McErlean and M. Müllner, *Angew Chem Int Ed*, 2019, **58**, 1828–1832.

73 J. J. Lessard, G. M. Scheutz, A. B. Korpusik, R. A. Olson, C. A. Figg and B. S. Sumerlin, *Polym Chem*, 2021, **12**, 2205–2209.

74 J. J. Piane, L. E. Chamberlain, S. Huss, L. T. Alameda, A. C. Hoover and E. Elacqua, *ACS Catal*, 2020, **10**, 13251–13256.

75 J. B. Deshpande, G. R. Navale, M. S. Dharne and A. A. Kulkarni, *Chem Eng Technol*, 2020, **43**, 582–592.

76 K. Bell, S. Freeburne, M. Fromel, H. J. Oh and C. W. Pester, *J Polym Sci*, 2021, **59**, 2844–2853.

77 M. Yuan, L. Xu, X. Cui, J. Lv, P. Zhang and H. Tang, *Polymers*, 2020, **12**, 1–12.

78 R. N. Carmean, M. B. Sims, C. A. Figg, P. J. Hurst, J. P. Patterson and B. S. Sumerlin, *ACS Macro Lett*, 2020, **9**, 613–618.

79 N. D. Dolinski, Z. A. Page, E. H. Discekici, D. Meis, I. H. Lee, G. R. Jones, R. Whitfield, X. Pan, B. G. McCarthy, S. Shanmugam, V. Kottisch, B. P. Fors, C. Boyer, G. M. Miyake, K. Matyjaszewski, D. M. Haddleton, J. R. de Alaniz, A. Anastasaki and C. J. Hawker, *J Polym Sci A Polym Chem*, 2019, **57**, 268–273.

80 Q. Fu, K. Xie, T. G. McKenzie and G. G. Qiao, *Polym Chem*, 2017, **8**, 1519–1526.

81 M. B. Perez, M. Cirelli and S. de Beer, *ACS Appl Polym Mater*, 2020, **2**, 3039–3043.

82 E. A. Smith and W. Chen, *Langmuir*, 2008, **24**, 12405–12409.

83 M. Li, M. Fromel, D. Ranaweera and C. W. Pester, *Macromol Rapid Commun*, 2020, **41**, 2000337.

84 R. A. Olson, J. S. Levi, G. M. Scheutz, J. J. Lessard, C. A. Figg, M. N. Kamat, K. B. Basso and B. S. Sumerlin, *Macromolecules*, 2021, **54**, 10, 4880-4888.

85 K. S. Padon and A. B. Scranton, *J Polym Sci A Polym Chem*, 2001, **39**, 715–723.

86 C. A. Ghiron and J. D. Spikes, *Photochem Photobiol*, 1965, **4**, 5, 901-905.

87 G. Manivannan, S. Semal, R. Changkakoti and R. Lessard, *Appl Phys B,* 1994, **58**, 73-77.

88 L. S. Herculano, L. C. Malacarne, V. S. Zanuto, G. V. B. Lukasievicz, O. A. Capeloto and N. G. C. Astrath, *J Phys Chem B*, 2013, **117**, 1932–1937.

89 P. Krys and K. Matyjaszewski, *Eur Polym J*, 2017, **89**, 482–523.